 ICCES, vol.5, no.1, pp.41-46

Intersection of Slender Longitudinal Vortices by Shock Waves

E. Krause[1], W. Schröder[1], M. Klaas[1], O. Thomer[1]

Summary

In supersonic flow the leading edge vortex of delta wings can encounter intersection by an oblique or a normal shock. The resulting interaction between the two influences the aerodynamic forces, in particular the lift, especially if vortex breakdown occurs. This problem was studied in an idealized form by assuming an isolated slender vortex being intersected by an oblique and a normal shock, respectively. The investigation was carried out in two coordinated companion studies, one using numerical solutions of the Euler and Navier-Stokes equations, and the other experimental techniques, i. e. flow visualization methods, and Laser-Doppler and particle-image velocimetry. The measurements yielded profiles of the axial and azimuthal velocity components of the undisturbed vortex, distributions of the axial velocity component, visualizations of the shock deformation, and the deflection of the vortex core for the case of the oblique-shock-vortex interaction. The numerical solutions yielded detailed profiles of all flow quantities including those of vortex breakdown.

Introduction

The problem indicated in the title is encountered in supersonic flight on delta wings, and on delta wings with leading-edge extension, when the primary vortex is intersected by a strong shock that may be generated near the trailing edge [1]. On canard configurations the vortex originating on the front aileron can interact with a shock on the main wing. Depending on the strength of the shock, the vortex can break down, and, due to the increase of the pressure in the core, rolling motions of the aircraft may set in as a direct result of the local loss of lift, or severe vertical tail buffeting may result, caused by the burst part of the vortices. This problem was extensively studied in experimental investigations, primarily for military applications. Reference [2], for example, may be consulted for details.

Although additional examples could be given, those listed may suffice to point to the importance of the aerodynamic problems mentioned. Previous experimental investigations, for example the work reported in [3] and [4] provided invaluable results, there is, however, still a need for further studies, mainly since numerical simulation techniques and experimental methods could substantially be improved in recent years, and there is still a lack of fundamental knowledge.

Two companion investigations, relating to the topic in question, were carried out at the Aerodynamisches Institut of the RWTH Aachen: In them the intersection of an isolated slender vortex by an oblique and a normal shock was studied

[1] Aerodynamisches Institut, RWTH Aachen, D-52062 Aachen, Germany

experimentally [5] and numerically [6]. The restriction to an isolated vortex was introduced to make the implementation of the boundary conditions accessible for both, the numerical and also for the experimental study. In the following some of the major results will briefly be discussed.

The Experiment

The experiments were carried out in the supersonic and the trisonic wind tunnel of the RWTH Aachen. The cross-section of the test chamber of the supersonic tunnel measures 15×15 cm^2, and that of the trisonic tunnel 40×40 cm^2. Experiments were performed for Mach numbers $1.4 \leq Ma \leq 2.5$. The intersection of a slender isolated vortex with an oblique shock, its axis orientated in the direction of the main flow, was studied first. The vortex was generated with the model of a rectangular half wing with a diamond-shaped profile, mounted on the top wall of the tunnel. The oblique shock was generated with a wedge, extending over the entire width from one side wall to the other. The circulation of the vortex and the intensity of the oblique shock were controlled by changing the angle of attack of the wing and of the wedge. The experimental set-up is schematically depicted below in Fig. 1, taken from [5].

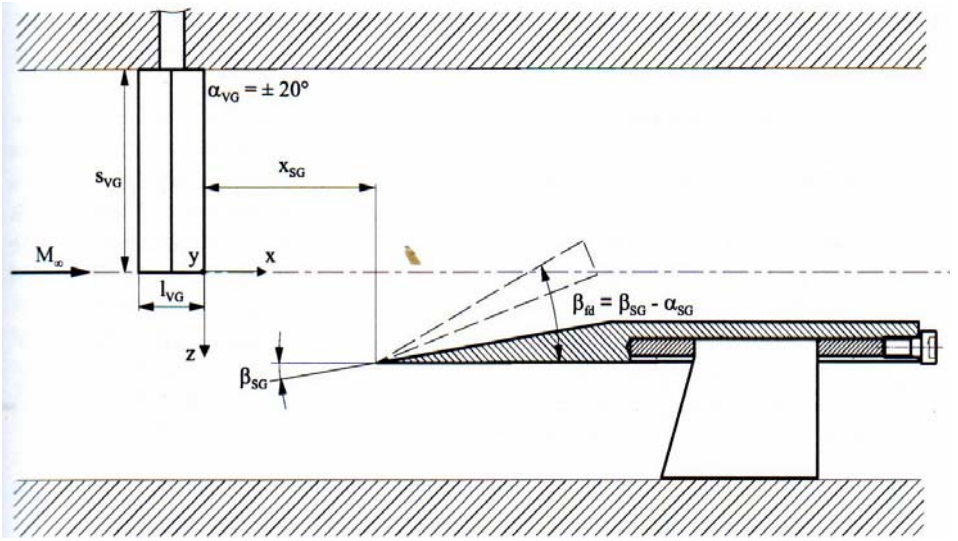

Figure 1: Schematic of experimental set-up for both wind tunnels used: The vortex generator, consisting of a rectangular half wing, with diamond-shaped profile (upper left part of Fig. 1), and the shock generator, consisting of an adjustable wedge (lower right part), from [5].

Velocity measurements and flow visualization studies were conducted in several measuring campaigns. In the first the undisturbed vortex was investigated by

measuring profiles of the circumferential and the axial velocity components in the supersonic wind tunnel at three stations downstream from the wing for several angles of attack with Laser-Doppler-velocimetry. The results confirm the typical rigid-body distribution of the circumferential velocity component and a wake-shaped profile of the axial component, although not axially symmetric.

In another campaign the intersection of the vortex by an oblique shock was studied in the trisonic tunnel with flow visualization and velocity measurements. The experiments consisted of two parts: In the first the flow was visualized with the standard and colored schlieren technique and differential interferometry, and in the second the velocity field was measured with the method of particle-image velocimetry in vertical planes downstream from the vortex generator. The following two pictures in Fig. 2 show typical results, obtained in the experiments of Ref. [5].

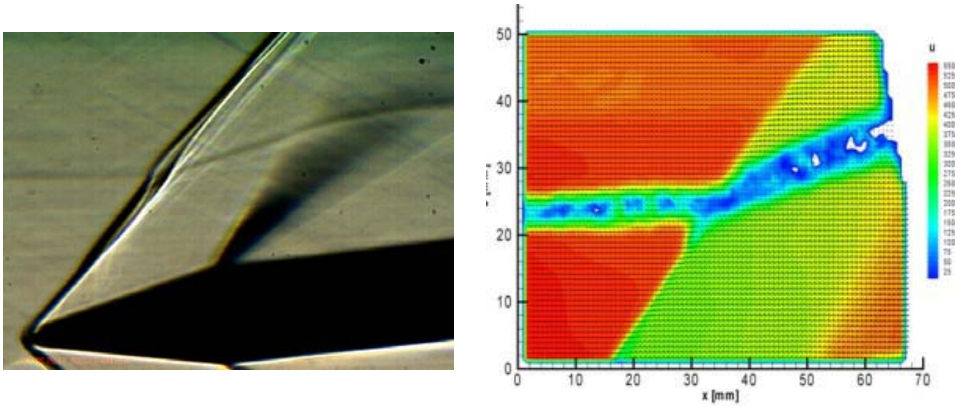

Figure 2: Intersection of a slender longitudinal vortex by an oblique shock at a Mach number $Ma = 2.2$, angle of attack of wing $\alpha_w = 6°$, and of the shock generator $\beta_s = 21°$; standard schlieren visualization on the left, particle-image-velocimetry results on the right, pictures were taken from [5].

The experimental results clearly reveal that the inclination of the shock is steepened by velocity non-uniformities in the vortex core. The shock takes on a slightly S-curved shape, recognizable in the schlieren picture. The particle-image-velocimetry measurements identify magnitude and direction of the velocity component projected on a vertical plane near the center of the vortex.

The experimental investigation of a normal shock intersecting a slender vortex has not been completed as yet. Results are expected in the near future.

The Numerical Work

For the numerical simulation of the problem solutions of the Euler and Navier-Stokes equations for time-dependent, compressible, three-dimensional, laminar flow

were used [6]. The time integration of the conservation equations was facilitated with a five-step Runge-Kutta method. The spatial derivatives of the convective fluxes were approximated with a node-centered finite-volume technique of second order to take into account their advective properties. All terms were approximated with the AUSM scheme of Liou and Steffen [7]. The integration was carried out in a rectangular computational domain, depicted in Fig. 3. Vortex and shocks are indicated in their representative initial position. Boundary conditions had to be prescribed on all bounding surfaces, and initial conditions in the entire domain.

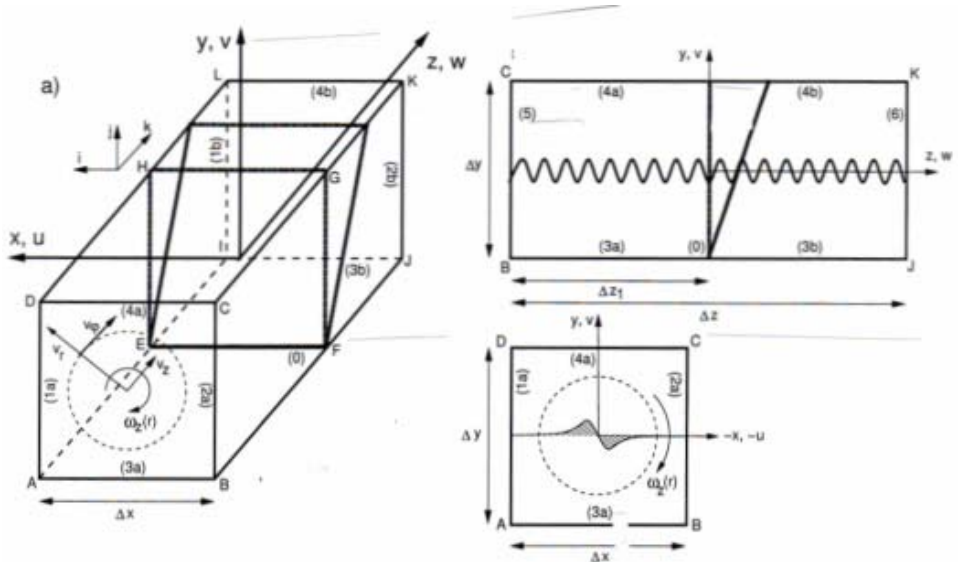

Figure 3: Computational domain for simulation of oblique- and normal-shock–vortex intersection, with initial position of shocks and vortex indicated [6].

The boundary conditions in the inflow cross-section were assumed to be given by a Burgers vortex, also used for the determination of the radial density and pressure profiles. In the outflow cross-section the non-reflecting boundary conditions of Poinsot and Lele [8] were prescribed for viscous flow simulation and those of Kevin and Thompson [9] for inviscid flow. The kinematic flow condition was implemented on the four bounding lateral surfaces, together with the Rankine-Hugoniot relations at a certain streamwise location on the bottom surface. For normal shock computations, the Rankine-Hugoniot relations were also imposed across the entire flow field, as an alternative, dividing the computational domain into two parts, with the Burgers vortex prescribed upstream of the shock. The initial conditions were approximated by the Burgers vortex used as boundary condition for the inflow cross-section.

Two examples of flow computations are discussed in the following. The first

relates to an experimental result, reported in [5]. In Fig. 4, the left picture shows a differential interferogram of an oblique shock intersecting a vortex at $Ma = 2.0$, generated by a wedge with $\beta_s = 11°$and the vortex generator at $\alpha = 6°$. The right picture shows lines of constant density in the vertical center plane of the computational domain, calculated with the numerical solution of the Navier-Stokes equations for the same flow conditions [6]. Both pictures show the S-curved shape of the originally straight shock, caused by the vortex.

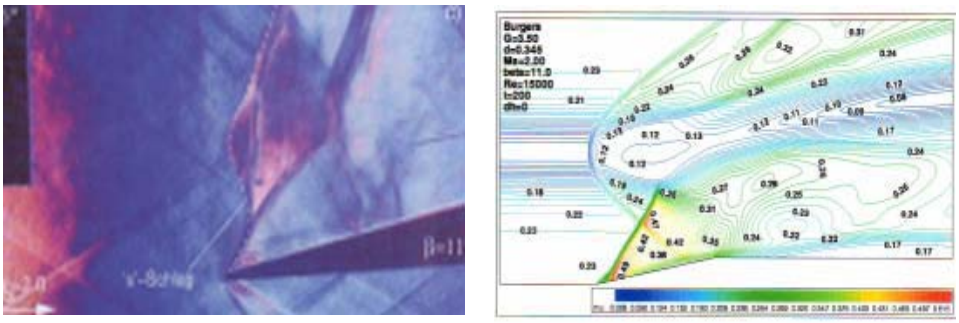

Figure 4: Vortex-oblique-shock intersection; photograph obtained with differential interferometry on the left (from [5]) and computed lines of constant density on the right (from [6]) show S-curved shape of the shock, caused by the vortex.

The second example shows streamlines in the horizontal center plane, computed for vortex-normal-shock intersection with Euler solution (left), and Navier-Stokes solution (right) [6].

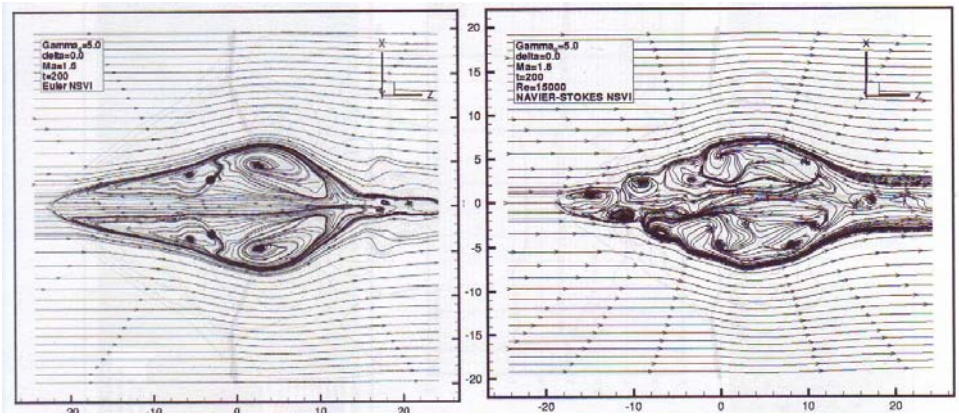

Figure 5: Computed streamlines for horizontal center plane of vortex-normal-shock interaction, Euler solution (left), Navier-Stokes (right); $Ma = 1.6$ [6].

The comparison of the results demonstrates that the Stokes stresses strongly affect the flow inside the recirculation region. Its conical shape hints at the distortion

of the originally straight normal shock: As details of the computational visualizations reveal, the shock adapts the form of a λ-shock.

Concluding Remarks

The intersection of slender longitudinal vortices by oblique and normal shock waves was investigated with experimental and numerical methods. The experiments yielded measurements of the axial and azimuthal velocity components and flow visualizations for the case of oblique-shock-vortex interaction. Results for normal-shock interaction with are not yet available. The results obtained in numerical solutions of the Euler and Navier-Stokes equations were compared. Detailed profiles of flow quantities were obtained, including the changes of the flow in the vortex core during breakdown and the associated deformation of the shock shape.

References

1. Krause, E. (2002): Axial Flow in Slender Vortices, *Journal of Engineering Thermophysics*, Vol. 11, pp. 229-242.
2. Lee, B. and Brown, D. (1990): Wind Tunnel Studies of F / A-18 Tail Buffet, *AIAA Paper No. 90-1432*.
3. Althaus, W. and Weimer, M. (1997): Review of the Aachen Work on Vortex Breakdown, in: *IUTAM Symposium on Dynamics of Slender Vortices*, Aachen, Aug. 3l-Sept. 3, (Krause, E., Gersten, K., Eds.), Kluwer Academic Pub., pp. 287-296.
4. Cattafesta, N. L. and Settles, G. S. (1992): Experiments on shock-vortex interaction, *AIAA Paper*, 92-0315.
5. Klaas, M. (2006): Experimental Investigation of Shock Vortex Interaction, Diss. Aerodyn. Inst., RWTH Aachen.
6. Thomer, O. (2003): Numerische Untersuchung der Wechselwirkung von Längswirbeln mit senkrechten und schrägen Verdichtungsstössen – ein Vergleich verschiedener Lösungsansätze, Diss. Aerodyn. Inst., RWTH Aachen.
7. Liou, M. and Steffen C. (1993): A New Flux Splitting Scheme, *Journal of Computational Physics,* 107, pp. 23-29.
8. Poinsot, T. and Lele, S. (1992): Boundary Conditions for Direct Simulations of Compressible Viscous Flows, *Journal of Computational Physics*, 101, pp. 104-129.
9. Kevin, W. and Thompson, K. W. (1990): Time Dependent Boundary Conditions for Hyperbolic Systems, l. c., 89. pp. 439-461.